Dynamics of the phase separation in solid solutions of ^{3}He-^{4}He

M. Bernier
Service de Physique du Solide et de Résonance Magnétique, Direction des Sciences de la Matière, CEA Saclay, F-91191 Gif-sur-Yvette CEDEX, France

P. Kumar
Department of Physics, University of Florida, Gainesville, Florida 32611
(Received 19 March 1991)

Measurements of NMR longitudinal and transverse relaxation times together with diffusion coefficients and pressure variations have been performed on solid solutions of helium-3 and -4 isotopes with ^{4}He concentrations $0<x_4<0.4$. All the measurements analyzed in the framework of a simple model follow the variation of the motion of ^{3}He atoms as a function of the x_4 concentration above the phase-separation temperature but also as the phase separation proceeds. In the mixed phase, the atomic motion appears to be sensitive to the quality and history of the crystal. Similar measurements have also been performed in a liquid mixture at $x_4=0.24$ as it phase separates.

I. INTRODUCTION

Many different techniques have been used to study the phase separation in solid helium mixtures.

(1) Specific heat measurements[1] of the mixtures exhibited a large change at the phase separation and could be fitted by the regular solution theory. The first diagram of the phase separation temperature T_{PS} as a function of the ^{4}He concentration x_4 thus obtained was found to be essentially symmetrical about $x_4=0.5$. This diagram was almost independent of the pressure of the sample for $P<70$ bars.

(2) Sensitive pressure measurements[2,3] were also used to measure the T-x_4 phase diagram and it remained close to the one deduced from specific heat measurements, but showed some asymmetry in $T_{PS}(x_4)$ for large x_4.[4]

(3) Sound velocity and attenuation measurements[5,6] performed in the solid solutions exhibit a hysteretic behavior after crossing the phase separation curve. This is attributed to the creation of dislocations when cooling through the phase separation which are annealed by warming the crystal to a temperature much larger than T_{PS}.

(4) A similar hysteretic behavior is observed in NMR experiments.[7] For temperatures above the phase separation, the spin lattice relaxation becomes nonexponential[8] suggesting a one-dimensional (1D) diffusion of the energy to relaxation centers (supposedly dislocations or ^{4}He atoms); the amplitude of the temperature hysteresis cycles for NMR and sound experiments is similar.

(5) A direct probe of phase separation is given by x-ray measurements monitoring the lattice spacing a in the crystal during a temperature cycle.[9] Various behaviors have been observed depending on the relative concentrations and the preparation of the sample; in several mixtures, the lattice spacing a decreases in the vicinity of the phase separation preceding a rapid change when the solution phase separates.

(6) Diffusion measurements using NMR also show[10] a phase separation dynamics depending on the history of the sample. However the diffusion coefficient D of the ^{3}He is unexpectedly high (comparable to D in the liquid phase) for solutions rich in ^{4}He and the diffusion seems quasi-one-dimensional. On the other hand the susceptibility measurements performed on the same sample give the usual Curie law.

(7) NMR measurements have also been performed in ^{4}He-rich samples looking at the modification of the atomic exchange rate with x_4[11] and to the growth speed of the separated phases in both high pressure (32 bars) and low pressure (28 bars) cases.[12]

Several of the puzzling features of the experiments mentioned above have been understood[13,14] but much remains to be done. Some questions of interest suggested by these experiments deal with the following.

(1) The possible existence of modulated structures in the vicinity of the phase separation.[15] This could be observed in NMR through boundary limited diffusion.

(2) The effect of fluctuations which are responsible for a short-range order above T_{PS} for 50:50 solutions.[14]

To have a better understanding of the dynamics of the phase separation we performed NMR measurements of the diffusion coefficient D of the ^{3}He atoms together with the spin lattice T_1 and the spin-spin T_2 relaxation times as a function of T on solid solutions of various relative concentrations whose pressure was continuously monitored during the experiment. The pressure of the sample was large enough to ensure that both isotopic phases would be solid but small enough to keep the diffusion coefficient in a measurable range.

We also performed the same measurements on a liquid mixture ($x_4\approx 24\%$) under its saturated vapor pressure in a temperature range where it phase separates.

We shall also comment on some minor observations made during the course of the experiments.

II. APPARATUS AND EXPERIMENTAL TECHNIQUES

The solid sample is prepared by a blocked capillary method in a cell made of Stycast 1266 (Fig. 1). The cell is placed inside the mixing chamber of a dilution refrigerator and is thermally coupled to the dilute mixture by 10 silver rods of diameter 0.6 mm. These rods are soldered to a silver plate embedded in sintered silver powder. The upper part of the cell also in contact with the silver rods is accessible to the dilute mixture and filled with fluorine DLX spheres of diameter 2000 Å.

The temperature is measured by several techniques.

(1) Carbon resistors are placed inside the mixing chamber. They are used as secondary thermometers and heaters to control the temperature of the mixing chamber.

(2) CW NMR of ^{19}F in the DLX spheres is also used as a secondary thermometer. Unfortunately in the dilute mixture the DLX spheres rapidly loose thermal contact with the liquid below $T=250$ mK and this secondary thermometer can only be used at high temperatures.

(3) A more direct measure of the temperature of the sample under study is deduced from the susceptibility of the solid solutions acting as a secondary thermometer.

The lower wall of the sample cell is the diaphragm of a Be-Cu strain gauge of standard design. The capacitor plates are enclosed in a chamber sealed at room temperature. The gauge is calibrated at low temperature (4.2 K) by filling the cell with liquid ^3He in pressure equilibrium with a room temperature volume whose pressure is measured by two reference gauges: a Sedeme CMB 200 strain gauge and a Digiquartz 2900AS pressure transducer. The pressure calibration is then used to calibrate the carbon resistors and ^{19}F NMR signals along the melting curve of solid ^3He in a magnetic field of 0.308 T corresponding to the experimental conditions. During the experiment the strain gauge monitors continuously the pressure of the sample kept at constant volume.

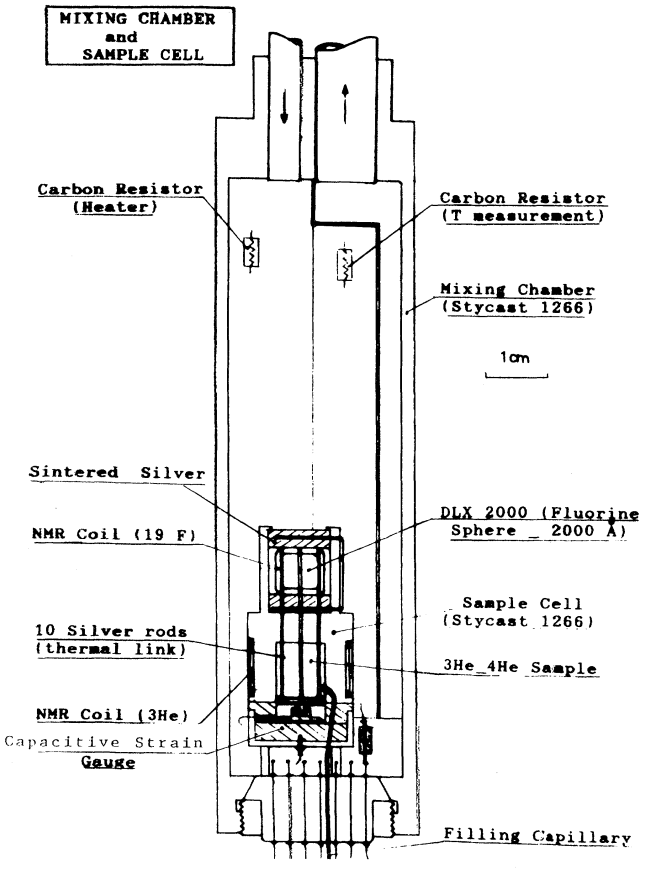

FIG. 1. Experimental cell and mixing chamber of the dilution refrigerator.

A superconducting magnet in persistent mode placed in the ^4He bath of the cryostat provides the necessary magnetic field. A superconducting solenoid wrapped around the outer copper shield of the dilution refrigerator allows us to adjust the DC field to the exact value for the pulse experiments or to sweep the field for CW experiments. A set of superconducting gradient coils located on the inner shield of the dilution refrigerator provides a field gradient of 3 mT/cm for 1-amp current necessary to measure the relatively small diffusion coefficients in our solid solutions.

Two NMR saddle coils are wrapped around the upper and lower parts of the experimental cell. Their axes are at right angles from each other to minimize any pick-up effect. The lines connecting the coils to the spectrometers are tuned to the chosen frequencies. Two separate NMR spectrometers are used for the experiments.

(1) A CW spectrometer at 12.3497 MHz is used for the NMR of ^{19}F spins. The detected signal is amplified and both plotted on a chart recorder and stored in a computer coupled to a high speed voltmeter Keithley 194A.

(2) A pulse spectrometer at 9.999 MHz coupled to a PC-AT computer is used for the NMR of ^3He spins in various magnetic field gradients. The block diagram is given in Fig. 2. An hp 8640B signal generator produces the radio frequency and the computer the required gate and pulse sequences. The pulses are amplified by two ENI linear amplifiers followed by a homemade class C power amplifier providing 1.1 kV peak to peak on the tank coil. The NMR signal is amplified and detected using a mixer driven by a reference signal from the signal generator with the proper phase shift. The signal is then read both by a digital storage oscilloscope Philips PM 3320A and by the high speed voltmeter Keithley 194A. It is then stored in the computer. A different procedure is also used, where the signal is not detected, to measure the magnetic field gradient by recording the zeros of the free precession more easily observed on a spin echo. This gives a direct measure of the magnetic field gradient in the experimental conditions.

We have studied five solid solution samples with ^4He concentrations x_4: 1.9×10^{-3}, 4.6×10^{-3}, 0.14, 0.24, 0.38 under pressures small enough to have measurable diffusion coefficients but large enough to ensure that the samples remain solid at any temperature, i.e., 35 bars $< P <$ 38 bars. These solids are bcc above the phase separation temperature T_{PS} in the mixed phase and the phase separation produces a bcc and an hcp phase at low

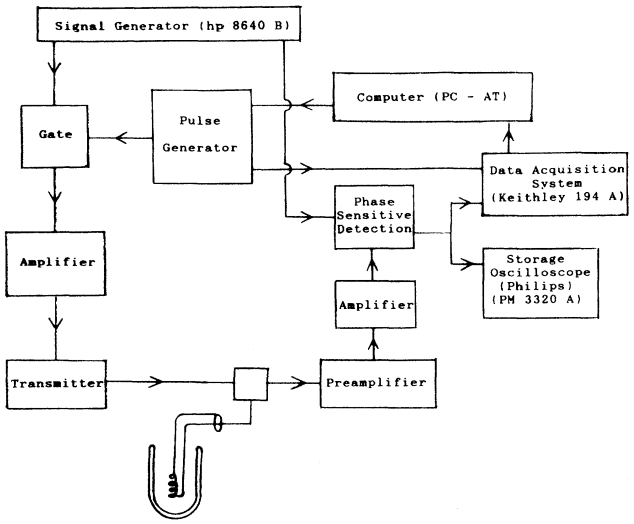

FIG. 2. Block diagram of the pulse spectrometer at $\omega/2\pi=9.999$ MHz used for the NMR of ^{3}He spins.

temperature.[3,13] The samples are annealed at high temperature (0.8–0.9 K) and then slowly cooled down to temperatures in the phase separation range.

The pressure of the sample is constantly monitored and we are able to see the excess of pressure due to the presence of vacancies at high temperature[16] and an increase when the temperature is lowered through T_{PS} (for $x_4 \geq 4.6\times10^{-3}$). We can thus locate the phase separation temperature. When T is further lowered below T_{PS} the pressure increases again during the cooling down and then relaxes slowly. On the other hand, when warming up starting from temperatures below T_{PS}, we observe a slow decrease of pressure as the ratio of the separated phases changes. Unfortunately a leak in the vacuum space of the strain gauge shifted the calibration of our pressure measurements and thus reduced their accuracy slightly. When the sample has reached equilibrium, we measure T_1, T_2, and D.

(1) The spin lattice relaxation T_1 is measured by the usual sequence of two 90° pulses.[17]

(2) The spin-spin relaxation time T_2 is measured by the Carr-Purcell sequence[18] using a 90° phase shift between the 90° pulse and the 180° pulses as suggested by Meiboom and Gill[19] to reduce the effect of inhomogeneity. We use a sequence of 43 pulses with a small spacing 2–10 msec) to reduce the effect of diffusion on the measurements.

(3) To measure the relatively small diffusion coefficients D ($\approx10^{-8}$ cm^2/sec) we need large magnetic field gradients (3 mT/cm for 1 amp in the coil). This also requires large RF pulses to rotate the spins as the gradient becomes comparable to the rotating RF field H_1. For our largest gradients, some correction is required. In order to look for the existence of diffusion barriers, a possible indication of modulated structures, we want to check if a single diffusion coefficient accounts for the dephasing of the spins both at short and long times. T_2 being often shorter than T_1, we use a stimulated echo technique sketched on Fig. 3 which keeps the echo bigger for longer times. The attenuation of the echoes following the usual 90–180 sequence and the stimulated echo sequence 90-90-90 is given by Eqs. (1) and (2),[20] respectively,

$$\ln\frac{M}{M_0}=-\frac{2\tau}{T_2}-\frac{2}{3}\gamma^2DG^2\tau^3\,, \tag{1}$$

$$\ln\frac{M}{M_0}=-\frac{(\tau_2-\tau_1)}{T_1}-\frac{2\tau_1}{T_2}-\ln2 \cdot-\gamma^2DG^2\tau_1^2(\tau_2-\tfrac{1}{3}\tau_1)\,, \tag{2}$$

where γ is the gyromagnetic ratio, M_0 and M, respectively, the nuclear signal amplitudes initially and at the time of the echo maximum. In our sequences we keep τ_1 constant and equal to 8 ms, which is much smaller than any of our T_2 values, and vary only $(\tau_2-\tau_1)$, the time period during which the signal relaxes with a characteristic time τ_1. We are thus able to measure the effect of diffusion for times of about 1 sec corresponding to diffusion over distances of the order of microns. A plot of $\ln M$ as a function of $(\tau_2-\tau_1)$, where τ_1 is small gives the characteristic relaxation rate of the echo which can be plotted as a function of G^2. The slope of the straight line gives the diffusion coefficient. The spin lattice relaxation time, obtained at $G=0$, can be compared to the usual measurement by a 90-90 pulse sequence.

It is worth pointing out a difficulty arising from the large magnetization of solid He at low temperature in a significant magnetic field and at a large molar volume where T_2 is a fraction of a second: this set of conditions produces "multiple echoes" in pulse sequences.[21] The type of pulse sequences used in this experiment is expected to minimize this effect due to the demagnetizing field acting on the spins during a time of the order of T_2.

We performed all the experiments reported hereafter with the same NMR spectrometer and were able to make relative comparisons of the susceptibilities of the samples.

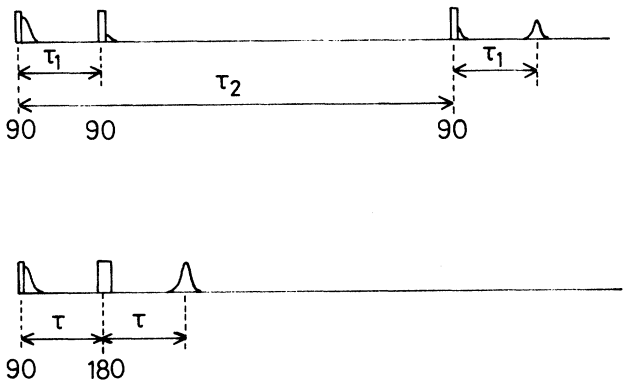

FIG. 3. Pulse sequences used for (a) conventional spin echo: 90-180, (b) stimulated echo: 90-90-90.

All solid samples followed a Curie law and the comparison of the various samples was a direct measure of the ^{3}He concentration of the solid solution. The amplitude of the free precession or of the echo allows us to measure *in situ* the average concentration x_4 of our samples at $G=0$, but we can also check the homogeneity of these samples by applying a field gradient which selects a slice of the cell, observed by NMR, the larger the gradient, the thinner the slice. The amplitude of the echo measured at short times for increasing values of G must remain constant for a homogeneous sample, after a small correction accounting for the decreasing efficiency of the pulse to rotate the spins in a high magnetic field gradient. This is essentially what we observe in our samples. The homogeneity on a smaller scale is also accessible in our experiments and we shall see that T_1 and T_2 and their variations are reproducible and less sensitive to the quality of the crystal than the diffusion coefficient of the ^{3}He atoms.

In most of our experiments we first anneal the crystal at high temperature and then cool down slowly. The time scale of a temperature change is a day and the time required to make a measurement of diffusion is 4 to 5 h as we allow the system to recover between pulse sequences.

Below T_{PS}, the solid has two components of different relative concentrations and we measure an average of their parameters.

III. EXPERIMENTAL RESULTS

In this section we report measurements of T_1, T_2, D, and the phase separation temperature deduced from our pressure data for five solid solutions with ^{4}He concentrations 1.9×10^{-3}, 4.6×10^{-3}, 0.14, 0.24, 0.38, and molar volumes differing by less than 1.5%. Except for a few data taken at high temperature (in the vicinity of 800 mK) where the number of vacancies is large, most of our NMR data are taken in a range where the relaxation times are only sensitive to the atomic exchange and independent of temperature; T_1 is a measure of the Zeeman-exchange relaxation and T_2 of the local field variations.[22,23]

In the following we consider each sample separately. Some of the samples have been cooled only once, but for some other concentrations several annealing and temperature cycles have been made and we shall comment on the results.

A. Solid solution of $x_4=1.9\times10^{-3}$ and $P=36.3$ bars

This sample with a low ^{4}He concentration can be directly compared to a number of former experiments made in almost pure ^{3}He.

Figures 4 and 5 give the experimental measurements of T_1, T_2, and D. We could not see a definite signature of the phase separation on the pressure gauge so that we can only assume T_{PS} from former experiments:[1-3,9] $T_{PS}=120$ mK. For this large molar volume and at a Larmor frequency $\omega/2\pi=9.999$ MHz, the NMR line is close to the extreme narrowing regime and T_1 is expected, on theoretical grounds, to be close to T_2. However, experimentally, the T_2 values are systematically about 30% less

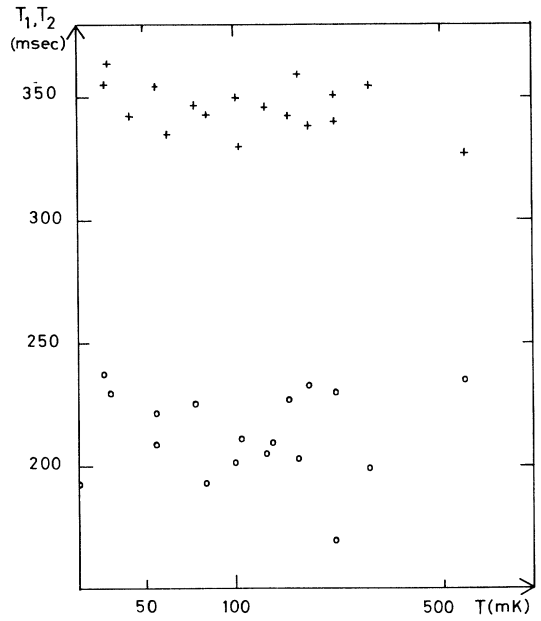

FIG. 4. Spin lattice $T_1(+)$ and spin spin $T_2(\circ)$ relaxation times as a function of temperature for a solid solution sample of $x_4=1.9\times10^{-3}$ and $P=36.3$ bars. (The spin lattice relaxation time T_1 plotted in the figure is the Zeeman-exchange relaxation time, T_{zex}. The long exchange-lattice relaxation time appearing at low temperature is not displayed.)

than the T_1 values for all the large molar volume experiments;[23] this is also true in the present case and our measurements are in good agreement with former results. As mentioned above, T_1, at high temperature, measures the Zeeman-exchange coupling and is temperature independent. When the temperature decreases, the exchange-

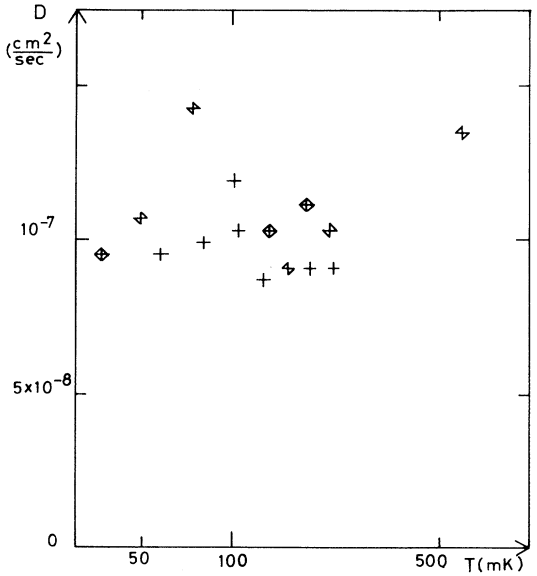

FIG. 5. Diffusion coefficient D as a function of temperature for a solid solution sample of $x_4=1.9\times10^{-3}$ and $P=36.3$ bars. Several cooling runs have been performed and are figured by different symbols.

lattice coupling also decreases and T_1 becomes a function of temperature and, as already observed in earlier experiments, becomes nonexponential in time (t) but exponential in the square root of the time ($\sqrt{t}$). This is consistent with a 1D diffusion process toward relaxing walls.[7,8] There is no visible sign of the phase separation on T_1 or T_2.

The diffusion coefficient is quite sensitive to the quality of the crystal. D is large at high temperature when there are many vacancies and decreases at lower temperature. A significant increase of D in the vicinity of the expected T_{PS} has been observed for two different cooling runs but our data points are too far apart in temperature to follow the detailed variation of D. Our figures for D are in good agreement with the expected values deduced from the "effective" exchange frequency in the crystal according to[24]

$$D_z = 4.12 \left[\frac{J}{2\pi} \right] a^2 .$$

At $V = 24$ cm^3/mole, using $J/2\pi$, given in Ref. 23, we obtain $D_z = 12 \times 10^{-8}$ cm^2/s to be compared with the experimental value $D \approx 9 \times 10^{-8}$ cm^2/s.

B. Solid solution of $x_4 = 4.6 \times 10^{-3}$ and $P = 37.8$ bars

One cooling run has been performed on this sample. The phase separation is observed on the pressure strain gauge by a slight increase at $T \approx 120$ mK. The measurements of T_1, T_2, and D given in Figs. 6 and 7 remain in the same range whether above or below the phase separation, and this is not too surprising as the ^{4}He concentration of the sample is low.

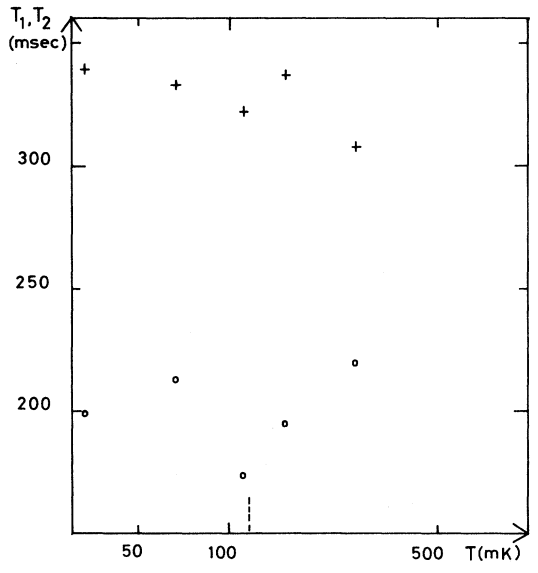

FIG. 6. Spin lattice $T_1(+)$ and spin spin $T_2(\circ)$ relaxation times as a function of temperature for a solid solution sample of $x_4 = 4.6 \times 10^{-3}$ and $P = 37.8$ bars. The phase separation temperature T_{PS} when cooling down is figured by a dashed line. (The spin lattice relaxation time T_1 plotted in the figure is the Zeeman-exchange relaxation time, T_{zex}. The long exchange-lattice relaxation time appearing at low temperature is not displayed.)

C. Solid solution $x_4 = 0.14$ and $P = 36.5$ bars

Several cooling runs have been performed on this sample after annealing the solid solution above 800 mK. The phase separation is observed on the strain gauge through a large increase of the pressure below 272 mK followed by a slow relaxation when the temperature is stabilized. From there on any decreases in temperature produces a new rise in pressure followed by a slow relaxation. Conversely warming up the phase separated solid produces a slow decrease in pressure. These pressure variations are significant only in the vicinity of the phase separation temperature; for much lower temperatures the change of pressure with temperature is very small.

Figures 8 and 9 give the experimental measurements of T_1, T_2, and D. As it is the case with purer samples T_1 and T_2 have similar behaviors, T_2 being smaller than T_1. Above T_{PS}, T_1 and T_2 are constant except for the higher temperatures ($T \approx 820$ mK) where the number of vacancies is large and increases the relaxation times. T_1 and T_2 increase when cooling through the phase separation to reach constant values corresponding to the relaxation times observed in samples of very low ^{4}He concentrations with the same molar volumes (cf. sample at $x_4 = 1.9 \times 10^{-3}$). The experimental measurements of the relaxation times do not seem dependent on the thermal cycling or the history of the sample and show no hysteresis as a function of temperature. This is true for T_1 and T_2 within the accuracy of our measurements.

The diffusion coefficient plotted in Fig. 9 exhibits a less simple behavior but the general features are similar for the various cooling runs. After annealing the crystal and cooling it to a region well above T_{PS}, D is relatively large but depends strongly on the quality of the crystal and

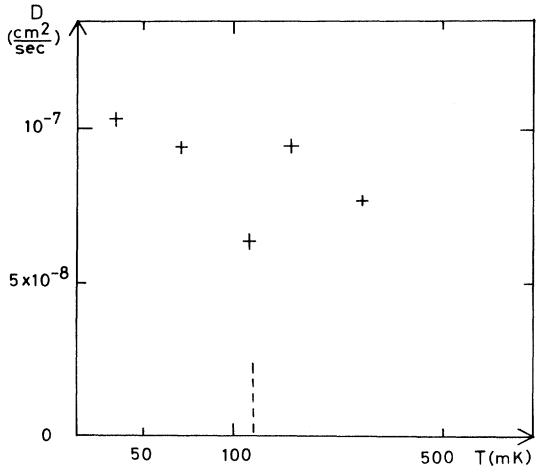

FIG. 7. Diffusion coefficient D as a function of temperature for a solid solution sample of $x_4 = 4.6 \times 10^{-3}$ and $P = 37.8$ bars. The phase separation temperature T_{PS} when cooling down is figured by a dashed line.

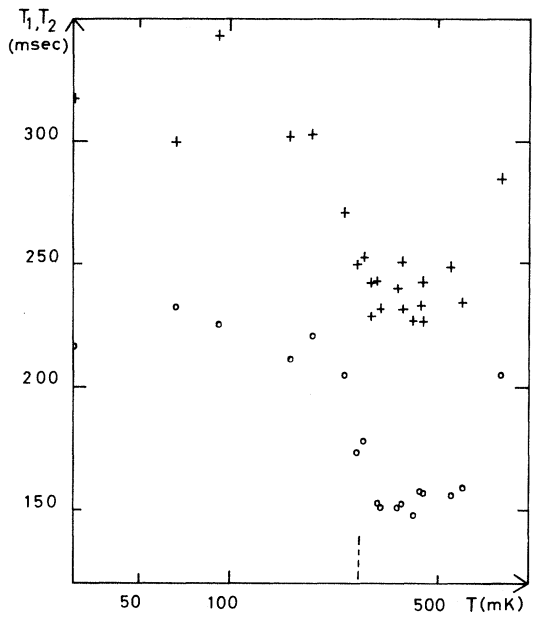

FIG. 8. Spin lattice $T_1(+)$ and spin spin $T_2(\circ)$ relaxation times as a function of temperature for a solid solution sample of $x_4=0.14$ and $P=36.5$ bars. The phase separation temperature T_{PS} when cooling down is figured by a dashed line. (The spin lattice relaxation time T_1 plotted in the figure is the Zeeman-exchange relaxation time, $T_{z\,ex}$. The long exchange-lattice relaxation time appearing at low temperature is not displayed.)

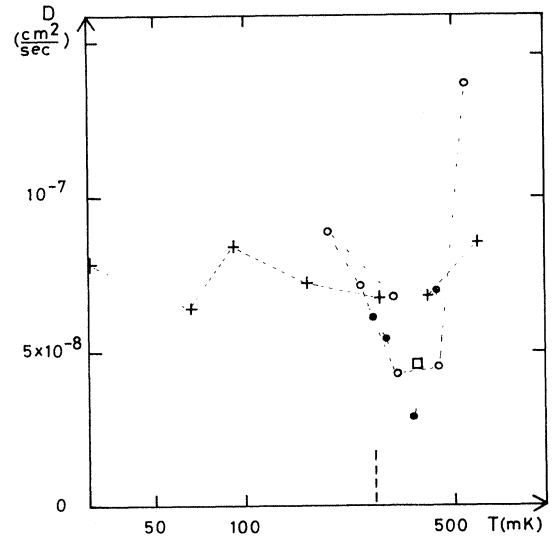

FIG. 9. Diffusion coefficient D as a function of temperature for a solid solution sample of $x_4=0.14$ and $P=36.5$ bars. Several cooling runs have been performed exhibiting the same general features and are figured by different symbols. The data taken during the same run are connected by straight lines. The phase separation temperature T_{PS} when cooling down is figured by a dashed line.

there is some scattering in the data. Reaching a temperature range above T_{PS} (where no variation of pressure is observed on the strain gauge) D decreases significantly and then rises again in the vicinity of the phase separation to reach a constant value below T_{PS}. The comparison of measurements taken on the same sample above the phase separation temperature before and after a cycling in the phase separated regime show an increase of D following the cycle.

Some unexpected features have also been observed in x-ray experiments in the same temperature regime close and above the phase separation. In some samples rich in ^{3}He, a decrease of the lattice constant, measured by x rays, precedes a large increase when cooling through this temperature range across the phase separation.[9] Both observations could be due to the creation of many defects, reducing the lattice spacing and slowing down the diffusion. It is worth noting that this is not observed for all of the samples of a given solid solution but seems to depend on the preparation history of the crystal.

D. Solid solutions at $x_4=0.24$, $P=35.2$ bars and $x_4=0.38$, $P=35.65$ bars

One sample of each solid solution was cooled down. Many of the features observed formerly were present.

In both cases a large variation of pressure followed by a slow relaxation was observed on the strain gauge when crossing T_{PS}. At $x_4=0.38$ the last two measurements were taken while warming up in the phase separation temperature range and a decrease of pressure was observed as expected. The pressure variation is always slower during a warm-up than during a cool-down.

The experimental measurements of T_1, T_2, and D are plotted in Figs. 10 and 11. T_2 in both cases is smaller at high temperature than in pure ^{3}He. It increases when the temperature decreases below T_{PS} to reach a plateau at low temperature corresponding to the value measured in samples of the same molar volume with very low ^{4}He concentrations (cf. sample at $x_4=1.9\times10^{-3}$). These are similar to the features reported at $x_4=0.14$. Below T_{PS} a single curve can describe the temperature dependence of the observed T_2 and no hysteresis in temperature is observed for $x_4=0.38$.

The behavior of T_1 is qualitatively different. As T_2, T_1 tends to a low temperature limit below T_{PS}, but the value above T_{PS} is not decreasing as x_4 increases as T_2 does. We have only a few data in this temperature range, but the trend is an increase of T_1 measured above T_{PS} as a function of x_4. We shall come back to this point later. As expected the low temperature limit of T_1 is close to the value in a sample of low ^{4}He concentration and of the same molar volume (cf. sample at $x_4=1.9\times10^{-3}$).

The measurements of D are plotted in Fig. 11 for both ^{4}He concentrations of the solid solutions. We have not enough data to study the detailed behavior of D in a temperature range close and above T_{PS}, but several characteristic features are noticeable. D is smaller in the homogeneous solution above T_{PS} than in the phase separated mixture and in that temperature range D is smaller when x_4 is larger. At $x_4=0.38$ the small value of D measured

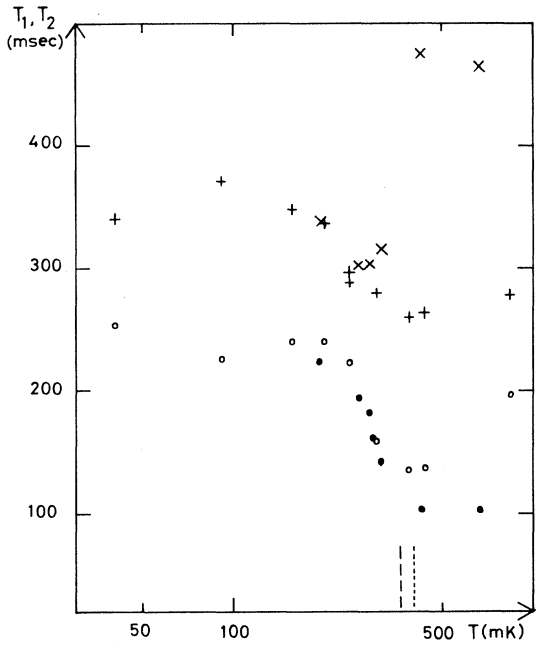

FIG. 10. Spin lattice T_1 and spin spin T_2 relaxation times as a function of temperature for two solid solution samples: (1) $x_4=0.24$, $P=35.2$ bars, $T_1(+)$, $T_2(\circ)$, the phase separation temperature T_{PS} when cooling down is figured by a dashed line. (2) $x_4=0.38$, $P=35.65$ bars, $T_1(\times)$, $T_2(\bullet)$, the phase separation temperature T_{PS} when cooling down is figured by a dotted line. (The spin lattice relaxation time T_1 plotted in the figure is the Zeeman-exchange relaxation time, $T_{z\,ex}$. The long exchange-lattice relaxation time appearing at low temperature is not displayed.)

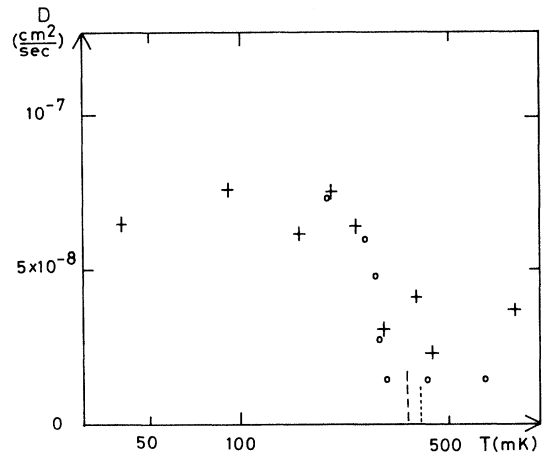

FIG. 11. Diffusion coefficient D as a function of temperature for two solid solution samples: (1) $x_4=0.24$, $P=35.2$ bars, $D(+)$, the phase separation temperature T_{PS} when cooling down is figured by a dashed line. (2) $x_4=0.38$, $P=35.65$ bars, $D(\circ)$, the phase separation temperature T_{PS} when cooling down is figured by a dotted line.

at $T>T_{PS}$ should be considered an upper limit of the diffusion coefficient which becomes difficult to measure and would require a larger magnetic field gradient to be determined with accuracy. As the temperature is lowered below T_{PS}, D increases and tends to a low temperature limit corresponding to the value expected in a sample of low ^{4}He concentration and of the same molar volume (cf. sample at $x_4=1.9\times10^{-3}$).

IV. DISCUSSION

Let us now compare the experimental measurements of T_1, T_2, and D obtained in solid solutions of $x_4\leq0.38$ and similar pressures. We shall, for the moment and for the sake of comparison, ignore the slight differences in molar volume. For all our samples the homogeneous solid solution lattice is supposed to be bcc.[3,13]

As expected, the three parameters tend to the limit of the ^{3}He rich sample at low temperatures ($T\ll T_{PS}$).

Above T_{PS}, D and T_2 decrease when x_4 increases while T_1 goes through a minimum as displayed in Fig. 12. In this temperature range and as mentioned before, the three parameters are independent of T and can be related to correlation functions of the atomic motion. The decrease of D for increasing x_4 indicates that the characteristic jump frequency of ^{3}He with ^{4}He atoms is lower than the ^{3}He-^{3}He one. Such a decrease in the atomic motion leads to a reduction of the motional narrowing and thus to a shortening of T_2 as observed experimentally.

To be more quantitative we need to make assumptions about the correlation functions. For a "pure" solid sample in the bcc phase, setting apart the largest molar volumes, the correlation function is known to be

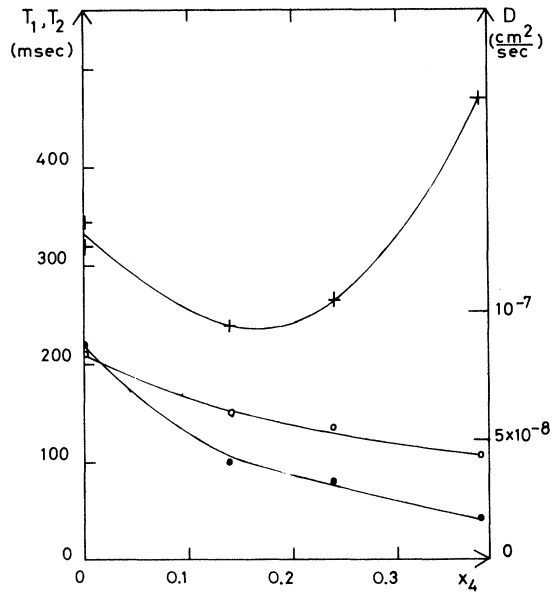

FIG. 12. Spin lattice $T_1(+)$, spin spin $T_2(\circ)$ and diffusion coefficient $D(\bullet)$ above the phase separation temperature plotted as a function of x_4. The solid lines are drawn as a guide to the eye.

Lorentzian giving an exponential spectral density, and we can calculate the expected values for T_1 and T_2 using as usual in NMR an average exchange frequency $(J/2\pi)$ to describe the various exchange motions inside the solid[22,23]

$$T_2^{-1}=\frac{\pi M_2}{3\omega_e}\left(\tfrac{3}{2}+\tfrac{5}{2}e^{-\omega/\omega_e}+e^{-2\omega/\omega_e}\right), \tag{3}$$

$$T_1^{-1}=\frac{\pi M_2}{3\omega_e}\left(e^{-\omega/\omega_e}+4e^{-2\omega/\omega_e}\right), \tag{4}$$

where $M_2=(2.274\times10^{11})/V^2$ is the second moment of the NMR line and ω_e is the characteristic modulation frequency of the dipolar field by atomic exchange and is proportional to the average exchange frequency:

$$\left[\frac{\omega_e}{2\pi}\right]\approx 3.38\left[\frac{J}{2\pi}\right].$$

As we mentioned above, this does not give a good description of the transverse relaxation behavior for large molar volumes in pure ^{3}He and the discrepancy is thought to be due to the spin diffusion in the inhomogeneous applied magnetic field.[23] For $V=24$ cm^3 with $J/2\pi=22$ MHz as reported in Fig. 31 of Ref. 23 Eqs. (3) and (4) give $T_1=288$ ms and $T_2=255$ ms which are consistent with our results.

When more ^{4}He is added to the sample, the correlation function for the modulation of the dipolar interaction should become similar to the one describing the modulation due to vacancy jumps. Such a correlation function, known for the relaxation in a high temperature regime, is exponential, giving a Lorentzian spectral density. The relaxation times can then be written

$$T_2^{-1}=\frac{2M_2}{3\omega}\omega\tau\left[\frac{3}{2}+\frac{5}{2}\frac{1}{1+\omega^2\tau^2}+\frac{1}{1+4\omega^2\tau^2}\right], \tag{5}$$

$$T_1^{-1}=\frac{2M_2}{3\omega}\omega\tau\left[\frac{1}{1+\omega^2\tau^2}+\frac{4}{1+4\omega^2\tau^2}\right], \tag{6}$$

where τ is a time characteristic of the ^{3}He jump. In a solid solution ^{3}He-^{4}He, the ^{3}He atoms are "diluted" and the second moment is proportional to the ^{3}He concentration $(1-x_4)$.[17] Therefore we can compare the experimental curves $T_2(1-x_4)$ and $T_1(1-x_4)$ as a function of x_4 with the parametric description given by Eqs. (5) and (6). The inverses of the right-hand sides of Eqs. (5) and (6) exhibit a dependence in $\omega\tau$ similar to the dependence in x_4 of $T_2(1-x_4)$ and $T_1(1-x_4)$. From the abscissa of the minima in the T_1 curves we can correlate $\omega\tau$ and x_4 and obtain $\omega\tau\simeq0.6$ for $x_4\simeq0.19$. We can then compare the experimental value of the minimum of $T_1(1-x_4)$ with the theoretical value deduced from Eq. (6) and also the experimental ratio T_1/T_2 to the theoretical one, both obtained without adjustable parameter. These quantities agree within 10%. Using a similar procedure we now compare the experimental and theoretical values of $T_1(1-x_4)$ and T_1/T_2 and adjust the $\omega\tau$ scale to obtain the best fit. The theoretical $\omega\tau$ values corresponding to the experimental x_4 appear in Fig. 13. This gives us a measure of the characteristic time for the ^{3}He atomic jumps and of its dependence on ^{4}He concentration in the lattice: changing the ^{4}He concentration x_4 by a factor of 2 from 0.19 to 0.38, changes $\omega\tau$, i.e., τ, by a factor of 3 from 0.6 to 1.8. As expected this description of the relaxation is only valid when the ^{4}He concentration in the solid solution becomes significant ($x_4\geq0.15$).

Knowing τ we can also estimate the diffusion coefficient in a random walk model. For $V=24$ cm^3 and $x_4\approx0.19$, $\tau\approx9.6\times10^{-9}$ sec and $D\approx2.4\times10^{-8}$ cm^2/sec while the experimental value of D interpolated from Fig. 12 is 3.3×10^{-8} cm^2/sec. As we just mentioned, increasing x_4 by factor 2 increases τ by a factor 3 and decreases D by a factor larger than 2 (our measurement is an upper limit of D at $x_4=0.38$). Keeping in mind the approximations we made these considerations show the good description of the experimental results given by this simple model.

In most of our experiments we could observe the stimulated echo for times up to 800 ms to 1 sec and the relaxation could always be described by a single exponential law thus excluding any possibility of boundary limited diffusion in our concentration range whether above or below the phase separation.

The time required for a typical diffusion measurement was of the order of 3 to 5 h during which the temperature but also the sample must remain stable. We have noticed that, although the stability of the measurement was very dependent on the sample, we usually had more scattering in the data above the phase separation temperature and this could not always be attributed to a smaller signal.

V. DIFFUSION IN LIQUID MIXTURES

Using the same setup we also performed T_1, T_2, and D measurements on a liquid mixture at "zero" pressure (the cell was full of liquid and the capillary was closed at the

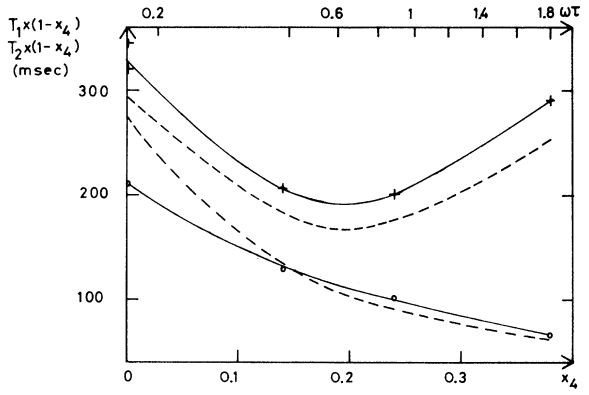

FIG. 13. Comparison of the experimental values of $T_1(1-x_4)$, (+), and $T_2(1-x_4)$, (○), plotted as functions of x_4 and figured by solid lines with their theoretical values deduced from Eqs. (5) and (6) plotted as functions of $\omega\tau$ and figured by dashed lines. The theoretical model is only valid for significant values of $x_4(x_4\geq0.15)$.

top of the cryostat). The ^{4}He concentration of the mixture was $x_4=0.24$. Except for the first measurement taken at high temperature in a homogeneous mixture, all the data were taken at temperatures below the phase separation and the measurements give an average of the properties of the two separated phases.

The susceptibility exhibits the same Fermi-type behavior as for pure ^{3}He and levels off at low temperature as shown in Fig. 14.

The spin lattice relaxation time given in Fig. 15 is long and probably not due to an intrinsic mechanism but is consistent with wall relaxation after diffusion; we come back to this point below. The measured transverse relaxation time is of the order of 1 sec but, again is not believed to be an intrinsic T_2. It is probably also due to the large value of the diffusion.

The measured diffusion coefficient D is also plotted in Fig. 15. It increases as the temperature decreases and the phase separation proceeds. The results are in good agreement with values measured in pure ^{3}He.[25] This is expected when the temperature decreases since the mixture separates in two components: one rich in ^{4}He and the other, the larger component, almost pure ^{3}He.

Considering the typical value of D and the random walk model, a ^{3}He atom diffuses over a distance of the order of 2 mm in a time equal to T_1, this remains true at low temperature as D increases by a factor 5 and T_1 decreases by a factor 3. This distance when compared to the spacing (≈ 1.5 mm) of the Ag wires used to cool the sample shows that the relaxation time T_1 obtained in our measurements is due to a wall relaxation.

VI. CONCLUSION AND PERSPECTIVES

The dynamics of the phase separation of solid solutions of helium isotopes ($x_4 \leq 0.38$) has been studied by NMR and pressure measurements for large molar volume samples. The spin lattice and transverse relaxation times do not show hystersis and are not very sensitive to the quality of the crystal while the diffusion coefficient can vary significantly with the history of the crystal above the phase separation temperature and large values of D have been measured at $x_4=0.14$. Above the phase separation temperature, T_2 and D decrease continuously when the ^{4}He concentration of the homogeneous solid solution increases showing a slowing down of the motion of ^{3}He atoms. For the same concentration range T_1 goes through a minimum and our measurements show that for $x_4>0.15$ the correlation function describing the motion of the ^{3}He atoms is close to an exponential, being thus very similar to the one describing the atomic jumps in a BPP-type or random walk model.[17,26] We then obtain the variation of the correlation time for the jump of ^{3}He atoms as a function of the concentration of ^{4}He in the solid solution. Below T_{PS} all the measured parameters tend to the values corresponding to a ^{3}He rich solid, as expected.

For larger ^{4}He concentrations several new features can be expected in the same type of measurements.

(1) In the vicinity and below the phase separation temperature, spatially modulated structures could form and lead to a boundary limited diffusion, a direct measure of the size of the structures.

(2) For solid solutions close to the critical point, i.e., $x_4 \approx 0.5$ a cooling down through the phase separation might show an increase of time constants and coherence

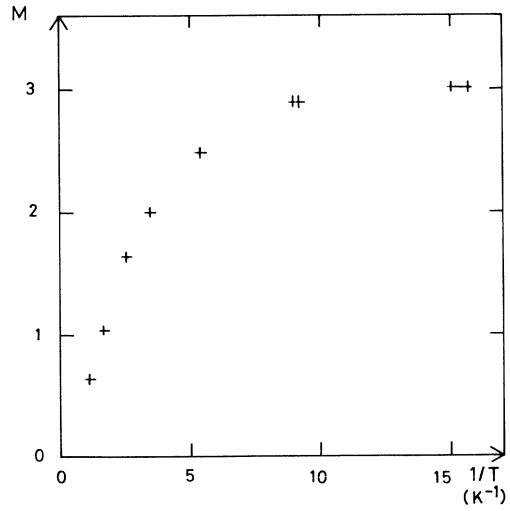

FIG. 14. Magnetization M of the liquid mixture with $x_4=0.24$ at low pressure plotted in arbitrary units as a function of the inverse temperature.

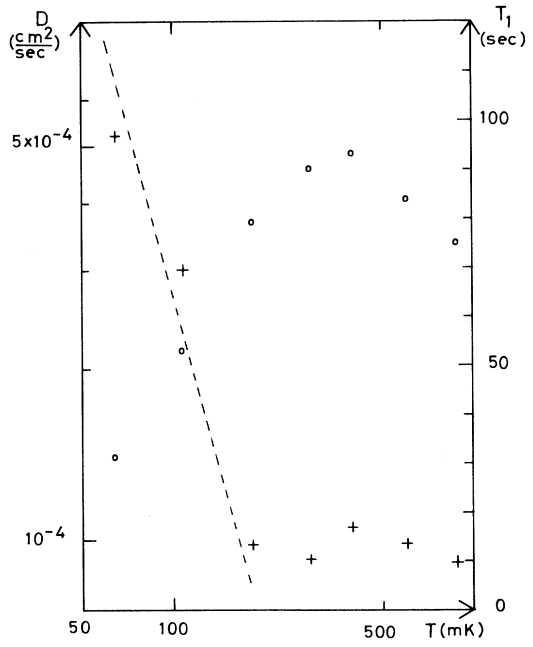

FIG. 15. Spin lattice relaxation time T_1(○) and diffusion coefficient D(+) for a liquid mixture with $x_4=0.24$ at low pressure plotted as a function of temperature. The dashed line figures a T^{-2} dependence of D as a function of temperature.

length in the solid, a critical slowing down leading to a decrease of D in the vicinity of T_c which has never been observed in a solid.[27]

We also report a series of measurements of T_1, T_2, and D in a liquid mixture at $x_4=0.24$. The phase separated mixture rich in ^{3}He exhibits a Fermi-type susceptibility and a diffusion coefficient rapidly increasing when T decreases. The relaxation times, although long, are not intrinsic but due to diffusion and wall effects.

ACKNOWLEDGMENTS

One of us (M.B.) would like to thank G. Guerrier for his technical assistance, M. Goldman for helpful discussions and his critical reading of the manuscript, and the University of Florida for its hospitality, partially supported by NATO Grant No. 88-703, during the latest stage of this work. The work of one of us (P.K.) was supported by National Science Foundation–Institute for Nuclear Theory (NSF-INT) Grant No. 8815199.

[1]D. O. Edwards, A. S. McWilliams, and J. G. Daunt, Phys. Rev. Lett. **9**, 195 (1962).

[2]M. F. Panczyk, R. A. Scribner, J. R. Gonano, and E. D. Adams, Phys. Rev. Lett. **21**, 594 (1968).

[3]P. M. Tedrow and D. M. Lee, Phys. Rev. **181**, 399 (1969); **187**, 398 (1969).

[4]W. J. Mullin, Phys. Rev. Lett. **20**, 254 (1968); **20**, 1550 (1968).

[5]I. Iwasa, N. Saito, and H. Suzuki, J. Phys. (Paris) colloq. **42**, C5-37 (1981).

[6]J. Beamish and J. P. Franck, Phys. Rev. B **28**, 1419 (1983).

[7]M. Bernier and G. Guerrier, Physica B **121**, 202 (1983).

[8]M. Bernier and G. Deville, J. Low Temp. Phys. **16**, 349 (1974).

[9]B. A. Frass, Ph.D. thesis, University of Illinois at Urbana-Champaign, 1980; S. N. Ehrlich, Ph.D. thesis, University of Illinois at Urbana-Champaign, 1987.

[10]V. A. Mikheev, V. A. Maidanov, N. P. Mikhin, S. E. Kal'noy, and N. F. Omelaenko, Proceedings of the 18th International Conference on Low Temperature Physics, Kyoto, 1987 [Jpn. J. Appl. Phys. **26**, Suppl. 26-3, 2131 (1987)]; V. A. Mikheev, V. A. Maidanov, and N. P. Mikhin, Fiz. Nizk. Temp. **12**, 658 (1986) [Sov. J. Low Temp. Phys. **12**, 375 (1986)].

[11]A. S. Greenberg, Ph.D. thesis, Material Science Center, Cornell University, 1971.

[12]N. Alikacem and M. G. Richards, in *Symposium in Quantum Fluids and Solids-1989,* Proceedings of Conference on Quantum Fluids and Solids, edited by Gary G. Ihas and Uasumasa Takano, AIP Conf. Proc. No. 194 (AIP, New York, 1989), p. 301.

[13]D. O. Edwards and S. Balibar, Phys. Rev. B **39**, 4083 (1989).

[14]P. Kumar and M. Bernier, J. Low Temp. Phys. **79**, 1 (1990).

[15]A. G. Khachaturyan, Sov. Phys. Crystallogr. **10**, 248 (1965).

[16]M. Bernier and J. H. Hetherington, Phys. Rev. B **39**, 11 285 (1989).

[17]A. Abragam, *The Principles of Nuclear Magnetism* (Clarendon, Oxford, England, 1961).

[18]H. Y. Carr and E. M. Purcell, Phys. Rev. **94**, 630 (1954).

[19]S. Meiboom and D. Gill, Rev. Sci. Instrum. **29**, 688 (1958).

[20]J. E. Tanner, J. Chem. Phys. **52**, 2523 (1970).

[21]M. Bernier and J. M. Delrieu, in *Proceedings of the XIX Congress Ampere, Heidelberg, 1976,* edited by H. Brunner, K. H. Hausser, and D. Schweitzer (Groupement Ampere, Heidelberg-Geneva, 1976), p. 127; G. Deville, M. Bernice, and J. M. Delrica, Phys. Rev. B **19**, 5666 (1979).

[22]A. Landesman, Ann. Phys. (Paris) **8**, 53 (1973); M. G. Richards, Adv. Magn. Res. **5**, 305 (1971).

[23]R. A. Guyer, R. C. Richardson, and L. I. Zane, Rev. Mod. Phys. **43**, 532 (1971).

[24]A. Redfield and W. N. Yu, Phys. Rev. **169**, 443 (1968); **177**, 1018 (1969).

[25]A. C. Anderson, W. Reese, and J. C. Wheatley, Phys. Rev. **127**, 671 (1962); J. C. Wheatley, in *Quantum Fluids,* edited by D. F. Brewer (North-Holland, Amsterdam, 1966), p. 183.

[26]N. Bloembergen, E. M. Purcell, and R. V. Pound, Phys. Rev. **73**, 679 (1948); H. C. Torrey, *ibid.* **92**, 962 (1953); **96**, 690 (1954); H. A. Resing and H. C. Torrey, *ibid.* **131**, 1102 (1963); M. Eisenstadt and A. G. Redfield, *ibid.* **132**, 635 (1963).

[27]Shang-Keng Ma, *Modern Theory of Critical Phenomena* (Benjamin, New York, 1976); H. Meyer, G. Ruppeiner, and M. Ryschkewitsch, *Proceedings of Dynamical Critical Phenomena and Related Topics, Geneva, 1979,* Lecture Notes in Physics Vol. 104 (Springer-Verlag, Berlin, 1979), p. 172.